Vol. 04, Iss. 2 (2026) 216-234, DOI: 10.61552/JME.2026.02.008

Journal of Materials and Engineering

www.jme.aspur.rs

Dielectric/Metal/Dielectric Thin Films for Flexible Solar Cell Cooling: Materials and Fabrication Technologies

Lalit Jyani[a,*], Khushboo Shah[a], Milind Kumar Sharma[a]

[a]*Centre of Excellence for Non-Conventional Energy, M.B.M. University, Jodhpur, Rajasthan, India.*

Keywords:

Passive cooling
Selective filters
Dielectric
Flexible solar cells
Substrate

* Corresponding author:

Lalit Jyani
E-mail: Jyani.lalit809@gmail.com

Received: 2 March 2026
Revised: 8 April 2026
Accepted: 15 May 2026

A B S T R A C T

The paper reviews a novel concept employing spectrally selective films for the passive cooling of flexible solar cells. This involves controlling visible transmittance and reflecting infrared radiation, reducing overall temperature without additional weight or moving parts. Spectrally selective filters with dielectric layers (TiO_2, WO_3, ZnO, ZnS) combined with noble metal coatings (Ag, Au) allow visible light transmission while reflecting infrared radiation. The study examines Dielectric/Metal/Dielectric(D/M/D) films coated on glass and flexible substrates (PEN, PET). By varying parameters like thickness and refractive index, the optical properties of these films can be tailored for high visible transmittance (T_{vis}) and solar infrared reflectance (R_{si}). The significance of this review lies in bridging the gap in the literature related to passive cooling for flexible solar cells. The findings contribute to understanding and adopting flexible solar cell technology in portable electronics and wearable applications.

1. INTRODUCTION

1.1 Global Energy Scenario: Role of PV and Flexible Solar Cells

The fast depletion of non-renewable energy resources has increased the demand for alternative resources, and solar energy has emerged as a frontrunner and one of the most promising energy sources being used for different applications. It is estimated that the total global installed capacity of solar PV will exceed natural gas by 2026 and coal-based energy by the year 2027[1], as shown in Figure 1.

Flexible solar cells offer a promising alternative to conventional PV technology, enabling lightweight, cost-effective solar harvesting. These second-generation thin-film PVs are deposited on glass, plastic, or metal substrates using high-throughput methods like roll-to-roll printing, achieving 3–15% efficiency under standard conditions [2].

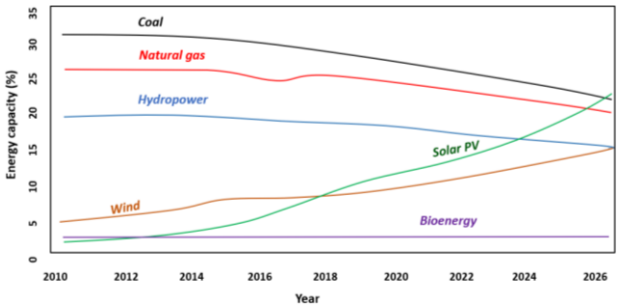

Fig. 1. Share of cumulative power capacity by technology, 2010-2027 [3]. Adapted with permission from the publisher.

Key types include amorphous silicon (α-Si), Copper Indium Gallium Selenide (CIGS), and Cadmium Telluride (CdTe), with the latter two rivaling crystalline PV efficiency [4]. Flexible PVs can be organic, inorganic, or hybrid, making them ideal for diverse applications. Figure 2 illustrates different flexible PV designs, including CIGS and CdTe structures, an actual CIGS device, an organic flexible cell, and material layer composition.

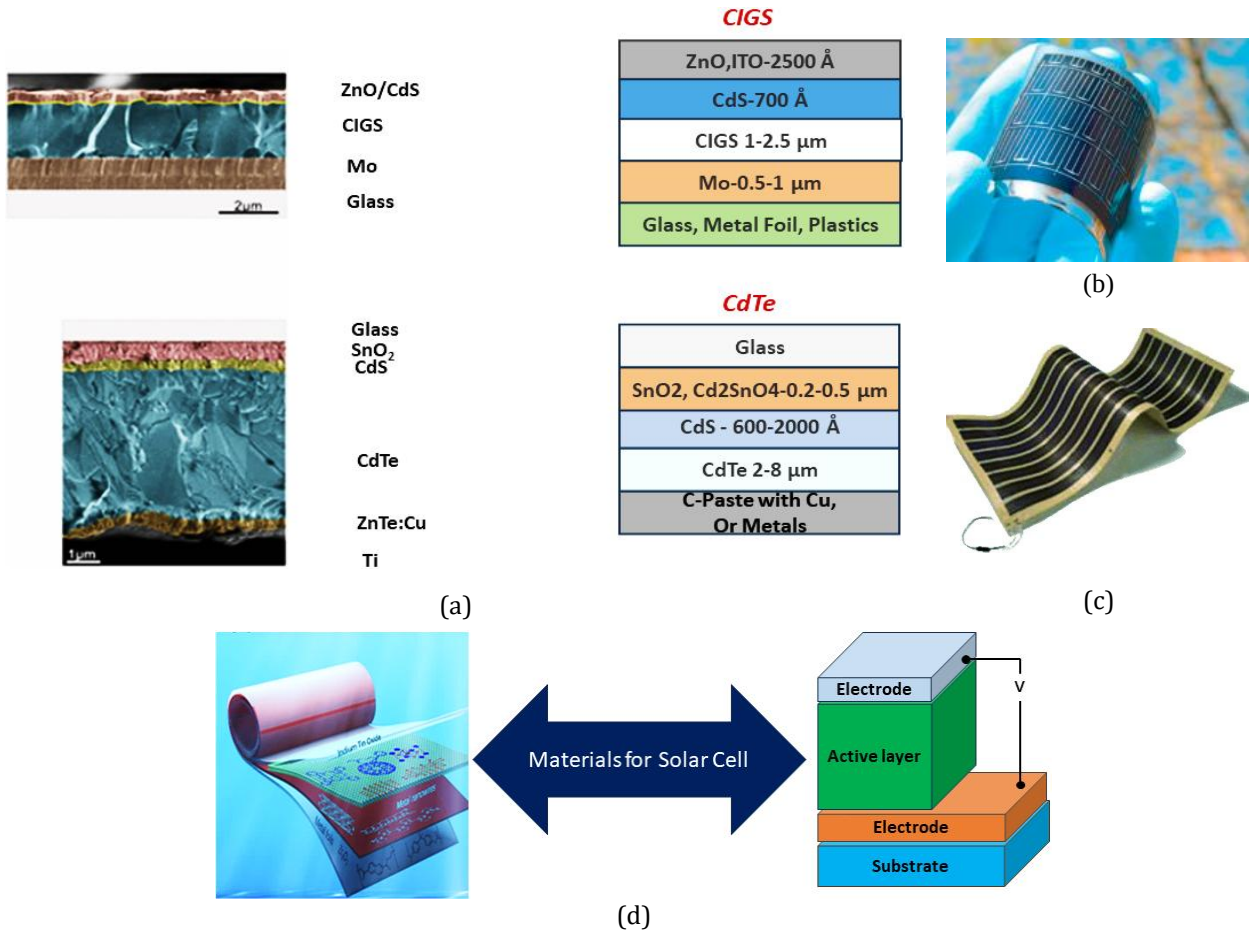

Fig. 2. (a) Comparative designs of thin film solar cells: CIGS and CdTe [5]. Pictures of a flexible (b) CIGS device on a plastic substrate [6](c) An organic flexible solar cell [3]and (d) Material layers of a flexible solar cell [7]**.** Adapted with permission from the publisher.

The various commonly used substrates for flexible PV are shown in Figure 3 with (a) their respective timelines of production and use over the last six decades. As can be seen, ceramic materials such as glass and Zirconia, and polymer-based materials such as PEN and Polycarbonate have been developed recently over the last few decades. In contrast, metals such as Molybdenum, Aluminium, Stainless Steel, and Titanium have been used for about 50-60 years.

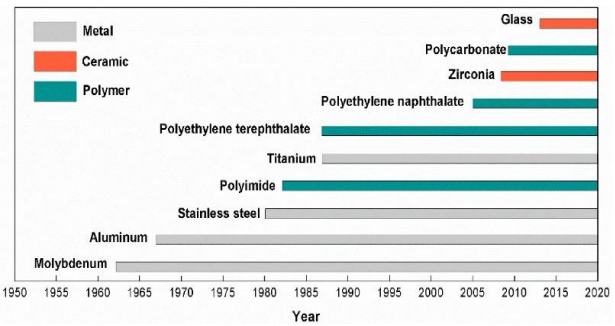

(a)

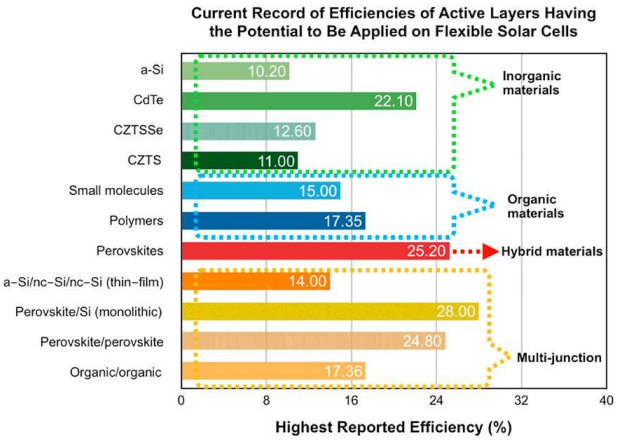

(b)

Fig. 3. (a) Some common substrates for flexible thin film solar cells: a historical view, and (b) Reported highest efficiencies of PV cells with various active materials, which have the potential for production on flexible substrates [7]. Adapted with permission from the publisher.

Figure 3 (b) compares the highest reported efficiencies of various active layers for flexible solar cells. Perovskite-based multi-junction and hybrid materials within the groups show the highest efficiencies in the region of 25-28 %.

The spectral impact on PV devices can be quantified using different indices; spectral response describes the sensitivity of the photosensor to optical radiation of different wavelengths. Some typical spectral response curves for PV technologies, given in Figure 4, show that the higher bandgap (a-Si, CdTe) technologies have a narrower SR-range compared to CIGS and conventional c-Si, and the absorption limit for a-Si and CdTe is closer to the visible region [8].

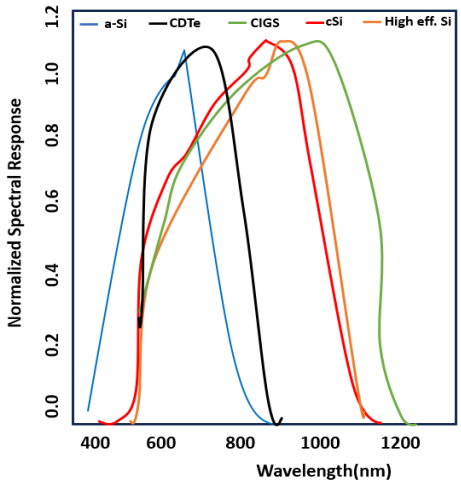

Fig. 4. Comparison of Conventional PV and Flexible Solar Cell technologies: Typical normalized spectral response curves [8]. Adapted with permission from the publisher.

According to Allied Market Research, the flexible thin film solar PV market size was valued at $ 464.31 m in 2020 and is projected to reach $914.07 m by 2030 globally, with a CAGR of 7.1% from 2021 to 2030 [9]. A comparative market assessment by application for 2020 and 2030 is shown in Figure 5.

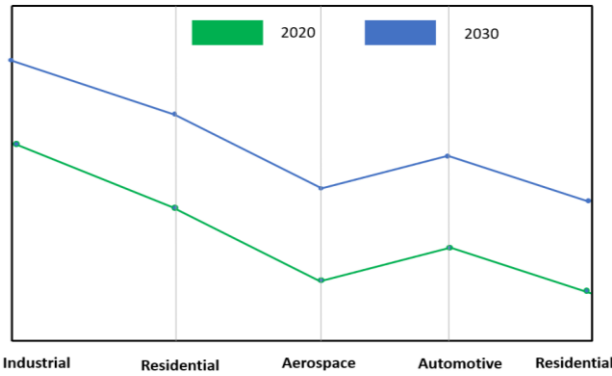

Fig. 5. Market Comparison by Application: Flexible Solar Panels between 2020 and 2030 [9]. Adapted with permission from the publisher.

1.2 Thermal Challenges with PV and Flexible Solar Cells

PV panels convert only a fraction of the incident radiation and have low conversion efficiencies (15-20%) [10]. More importantly, the efficiencies of the vast majority of PV converters drop when the temperature increases, with a rate commonly between -0.1 to -0.5% K^{-1}. This implies that for every 1°C rise in cell temperature, the efficiency will reduce by 0.1 to 0.5 % [11]. A diagrammatic example of the detrimental effects of temperature on the PV efficiency above the standard operating conditions from the available literature is shown in Figure 6. In Figure 6 (a) a typical Power-Voltage (P-V) curve for PV is plotted for temperatures up to 75°C. Figure 6 (b) shows the Current-Voltage (I-V) and the P-V curves for a specific type of mono-Si solar cell at a constant irradiance of 550 W/m^2 for cell temperatures of 25°C, 40°C, 50°C , and 60°C. In Figure 6 (c), the maximum experimental efficiency of a 14kW commercial PV panel with water cooling is depicted as the module temperature approaches the highest allowable temperature of 45°C.

As the conversion efficiency of the solar cell degrades with the rise in temperatures, an efficient cooling system is required to compensate for the efficiency losses caused by the increased surface temperatures. For crystalline silicon solar cells, every 1°C temperature rise leads to a relative efficiency decline of about 0.45% [3].

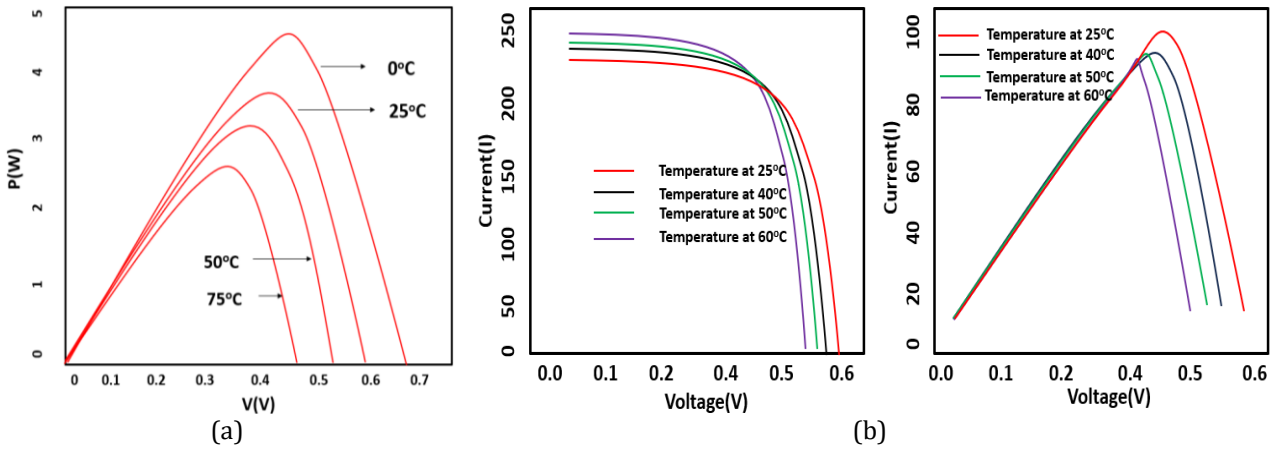

Fig. 6. The effect of module temperature on: (a) P–V curve for a typical PV (0-75°C)[11], (b) I-V and P-V curves for a mono-Si solar cell [12]. Adapted with permission from Publisher.

The fill-factors (FF) of the three key flexible solar cell technologies, namely, α-Si, CIGS, and CdTe, are shown in Figure 7, where, except α-Si, the other technologies show a proportional decrease in FF with the increase in temperature. The anomaly of α-Si is due to the Staebler-Wronski effect, in which a regenerative and beneficial effect occurs due to the annealing of the cell.

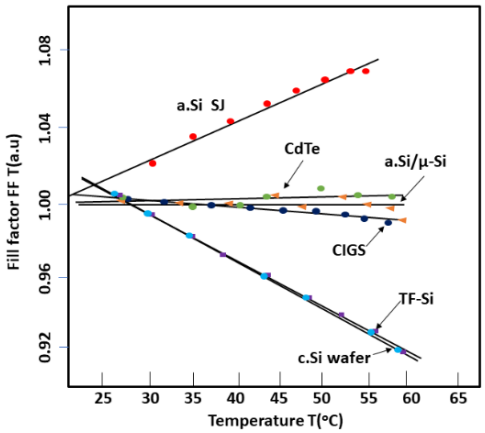

Fig. 7. Comparison of the fill factor of different thin-film flexible technologies as a function of temperature (experimental data) [4]. Adapted with permission from the publisher.

2. METHODS

Several cooling methods to reduce the operating temperature of solar PV are suggested in the literature that can be applied to the surface of the solar cells as depicted in Figure 8. These include both active (e.g. water cooling using a pump) [13, 14] and passive cooling techniques such as heatsinks and the use of phase change materials or PCM [15, 16]. As the passive cooling technologies consume no external power and does not add to the system bulk due to added components, this method is preferred to active cooling for flexible solar cells [11]. The authors in [17] have studied various passive cooling mechanisms for solar PV according to use and methods such as immersion cooling, heat pipes, natural air cooling with fins, heat sinks, and improved heat exchanger designs showed uniformity in operating temperatures.

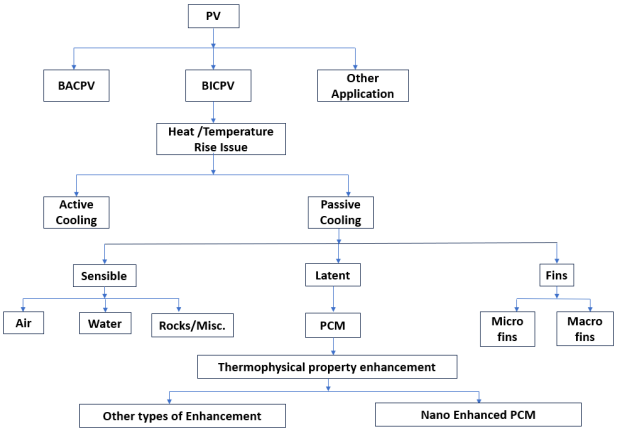

Fig. 8. Cooling methods for solar photovoltaic [17]. Adapted with permission from Publisher.

The passive cooling techniques, such as radiative cooling and spectral selective filtration of the incoming solar radiation, are discussed here.

2.1 Radiative cooling using DMD Filter

Passive radiative cooling has drawn much attention due to its potential application in cooling PV solar cells. It reflects solar radiation selectively and transmits in the PV conversion band (0.4-1.6 μm) to decrease the temperature of the system without consuming any energy [18]. A solar cell cannot convert sub-band-gap photons to electricity.

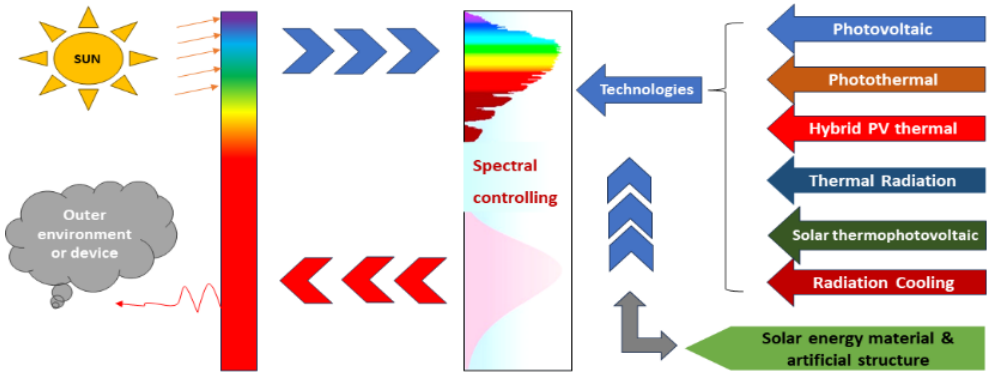

Fig. 9. Schematic diagram of energy harvesting and saving from the sun and the outer environment via spectral control [19](Adapted with permission from Publisher).

Practical solar cells exhibit sub-band gap absorption, generating parasitic heat rather than photocurrent [19]. Figure 9 illustrates spectral control technologies. Radiative cooling passively dissipates excess heat into the sky by reflection [18]. A blackbody's spectral radiation follows Planck's law, where emissivity (ε) equals absorptivity (α) at thermal equilibrium [20, 21]. The cosmic background (~3K) acts as a heat sink for solar cells [22]. Effective radiative cooling coatings should exhibit broad emissivity (3–20 μm) and high transmissivity (0.1–1.4 μm) [22]. Unlike terrestrial radiative cooling, which utilizes an 8–13 μm window, space-based cooling relies on emission within 3×10^{-5} mm and 8×10^{-13} mm [19]. High-emissivity coatings on flexible solar cells would benefit space applications. Various photonic strategies enhance radiative cooling by minimizing reflection losses (0.375–1.1 μm) and maximizing emissivity beyond 4 μm. An ideal radiative cooler reduces solar cell temperature by 18°C, improving efficiency by 7.9% [23]. A transparent silica-based cooler functioned as a blackbody in the mid-infrared range, enhancing performance [23]. A designed photonic structure enabled solar absorption while cooling the cell underneath it [24]. Mono-crystalline Si PVs benefited from radiative cooling and sub-bandgap reflection, reducing temperatures by ~10°C and increasing efficiency by ~6% compared to conventional cooling methods [25].

Figure 10 (a) depicts radiative cooling layers in silicon PVs. Figures 10 (b) and (c) compare absorptivity and emissivity for different material configurations, including encapsulated, bare, and EVA-coated cells.

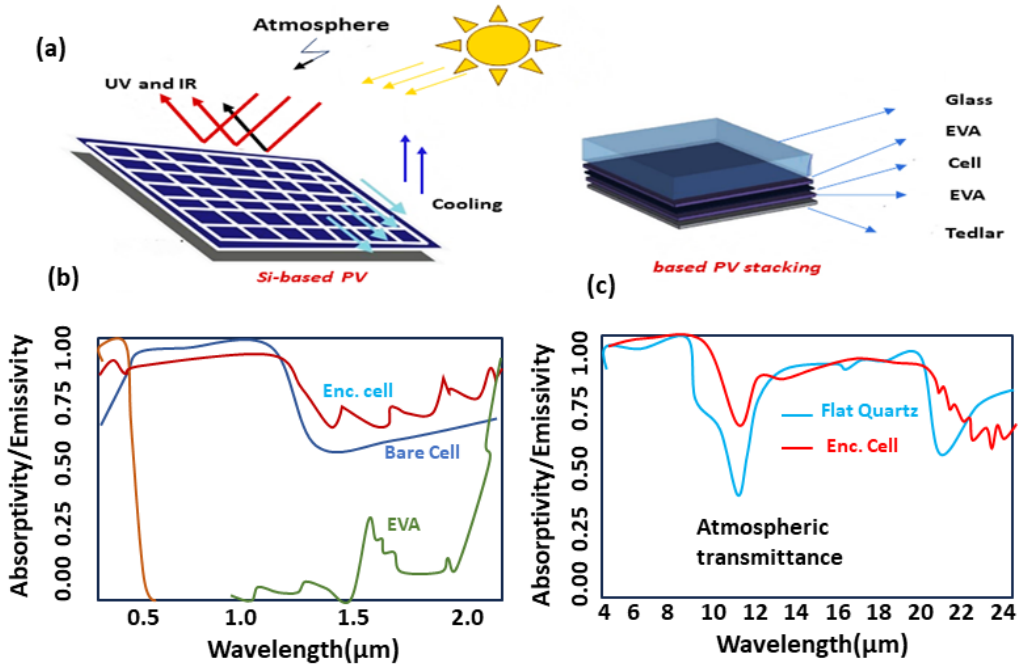

Fig. 10. (a) Radiative temperature regulation in Si-PV and the layers of an encapsulated crystalline Si-PV (b) Absorptivity/emissivity comparison of bare, encapsulated, and EVA wafers, and (c) Emissivity comparison of an encapsulated vs. fused Quartz glass [25] (Adapted with permission from Publisher).

The selective spectral response of solar cells enhances thermal emissions [23] while minimizing waste photon absorption [24]. Dielectric coatings (SiO2, TiO2, Si3N4, Al2O3) [26] and thin metal films (Ag, Au, Al) [27, 28] improve reflectance in the IR spectrum, reducing solar cell temperature. Dielectric/metal/dielectric (D/M/D) multilayers optimize transmittance in the visible range while reflecting IR radiation, as shown in Figure 11. This review analyzes D/M/D materials on glass and flexible substrates, highlighting their impact on passive cooling and electrical efficiency enhancement. Flexible solar cells cater to off-grid energy needs, benefiting soldiers, wearables, and portable power solutions. They can be integrated into helmets, jackets, tents, vehicles, and rooftops for extended solar harvesting. D/M/D coatings offer durable, transparent, low-emissivity layers crucial for future passive cooling applications. These material systems will continue driving energy-efficient PV solutions.

We discuss D/M/D coatings developed via chemical and physical vapor deposition, including sputtering, evaporation, and atomic layer deposition. The impact of material type, layer thickness, refractive index (n), and absorption coefficient (k) on transmittance and reflectance is analyzed. Emphasis is placed on applying D/M/D coatings to flexible PET substrates, optimizing their use for passive cooling in flexible solar cells where temperature control is crucial.

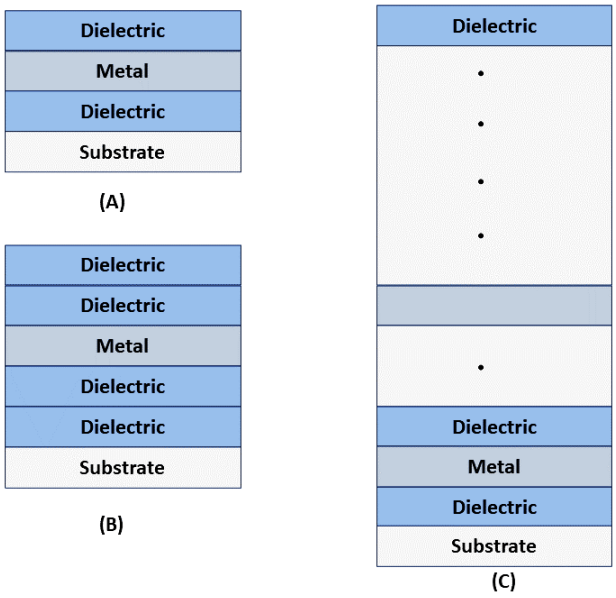

Fig. 11 A Schematic diagram of popular design structure types of DMD multilayer coatings [29]. Adapted with permission from the publisher.

As radiative cooling has certain limitations on solar cells whose encapsulated material already has high emission properties and acts like a radiative cooler, therefore a different approach for cooling solar cells is needed. Selectively filtering solar radiation by using multilayer photonic coolers with different materials of (SiO2), titanium dioxide (TiO2), silicon nitride (Si3N4), and aluminium dioxide (Al2O3), etc., is an effective passive cooling method for solar cells [24]. Simulations reveal that using multilayer materials coating over solar cells can increase effective photon transmittance and increase reflection of unwanted photons [30]. A well-designed photonic cooler could reduce the working temperature of solar cells by 5.7°C [30]. In literature [31], it was reported that cooling solar cells by spectrally selective filters is more effective compared with radiative cooling.

2.2 Spectral response of solar cells

The spectral response of solar cells spans ultraviolet (250-380 nm), visible (380-780 nm), solar infrared (780-2500 nm), and long-wave radiation (>3000 nm) [32, 33]. Spectrally selective filters play a key role in passive cooling by enhancing thermal emission, blocking IR radiation, and transmitting visible light. These filters eliminate waste photons that do not generate electron-hole pairs, reducing optical losses. Optimally designed filters transmit high-energy solar and near-infrared light (up to 2000 nm) while reflecting thermal infrared radiation into the atmosphere, thereby lowering the operating temperature of solar cells [33, 34].

2.3 Passive cooling using Dielectric / Metal / Dielectric coating

Dielectric/Metal/Dielectric (D/M/D) structures are highly effective as visible transparent solar infrared reflecting films, aiding in energy saving by transmitting visible light and reflecting solar infrared radiation [28]. Solar selective coatings exhibit spectrally dependent optical properties, enabling passive cooling by controlling incoming radiation. Dielectric coatings, composed of materials with strong ionic and covalent bonds, are transparent to visible and/or infrared light. Electromagnetic wave interaction in these coatings is explained by Maxwell's equations [35] and surface plasmonic resonance [36]. Micro-nanoscale structures influence permittivity and

optical properties through electromagnetic resonance, making photonic crystals crucial in optical filters due to their broad spectral tunability [37]. The schematic diagram of a metal-dielectric-metal structure is shown in Figure 12 (a) and consists of a bottom Ag layer, a middle SiO2 layer, and a top ultrathin silver (Ag) layer. The corresponding electric field maps in Figure 12(b) confirmed that an m-order Fabry–Perot resonance was generated in the SiO2 cavity at the wavelength of the absorption peaks. These peaks can shift quickly when the thickness of SiO2 changes.

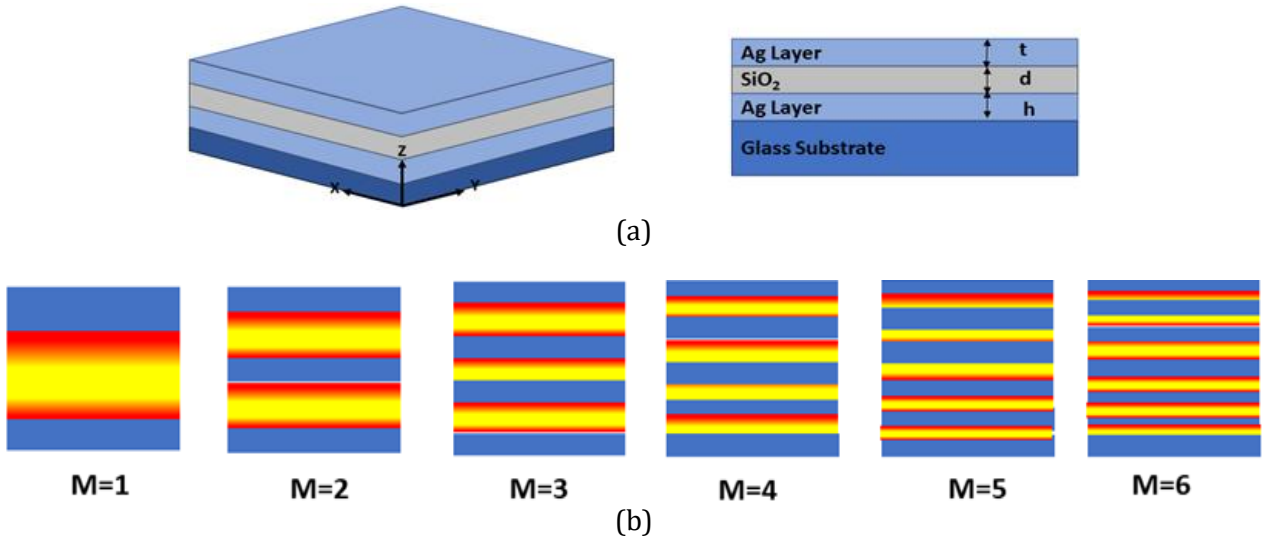

Fig. 12 (**a**) Schematic of a Metal-Dielectric-Metal (MDM) structure perfect absorber and (**b**) Variation in electric field distribution in the SiO_2 cavity at the absorption peaks from m = 1 to m = 6, where m is the mode [38]. Adapted with permission from Publisher.

2.4. Optical properties of dielectric and metal films

When the incident photons have a frequency that matches the energy needed to excite electrons to a higher allowed state, then the photons get absorbed. When the incoming radiation has photons, whose energy does not match the required excitation energy, no excitation occurs, and the material acts as transparent to incoming radiation. In nonmetals, the minimum energy separating the highest-filled electron states (valence band) and the lowest-empty electron states (conduction band) is known as the energy band gap. The transition of an electron from one band to another band constitutes the highest source of absorption.

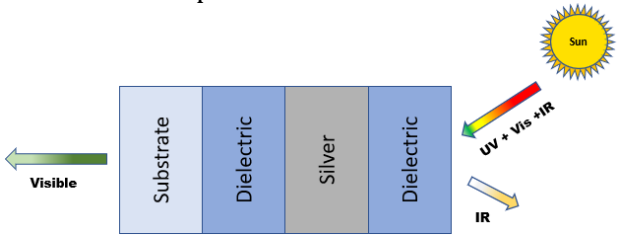

Fig. 13 Thin film multilayer Dielectric / Metal / Dielectric [21] (Adapted with permission from Publisher)

Dielectrics like glass, quartz, and metal oxides do not absorb visible light due to their high band gaps, with minimal reflection designed at 650 nm, where solar photon flux peaks [39]. Metals, in contrast, are highly reflective and opaque to visible and IR radiation due to free electron movement [35].

Silver, with the lowest optical losses from blue to near IR, is ideal for Low E coatings, offering a clear, color-neutral appearance [40]. Adding an antireflection (AR) dielectric overcoat reduces optical losses by minimizing reflection and protecting the metal layer [41, 42]. A well-designed D/M/D multilayer as shown in Figure 13, provides high visible transmittance and IR reflectance, lowering the solar cell's operating temperature.

3. MATERIALS

Dielectric/Metal/Dielectric (D/M/D) thin-film multilayers are extensively studied due to their applications in photonics, plasmonics, optics, energy generation, and optoelectronics. Silver-based D/M/D multilayers are prime candidates for heat mirror applications due to their high

visible (380-780 nm) transmittance and strong solar infrared (780-2500 nm) reflectance, essential for the passive cooling of solar cells [28, 43].

The thin metal layer, often made of noble metals like Ag, Cu, or Au, provides infrared reflection, while dielectric layers such as TiO2, WO3, ZnO, or ZnS enhance visible transmittance and act as surface passivation [14, 33, 44-46]. The spectral selectivity of these films depends on parameters like metal layer thickness, refractive index, and deposition technique [47, 48]. Table 1 summarizes D/M/D materials and their impact on visible transmittance and IR reflectance, while Table 2 provides their optical properties.

Table 1. Summary of D/M/D materials and their effect on maximum visible transmittance at different D/M/D layer thicknesses.

Materials (D/M/D)	Substrate	Max. Visible transmittance/ wavelength	Deposition technique	Reference
$WO_3/Au/WO_3$	Glass	84%/680nm	Thermal evaporation	[49]
$TiO_2/Ag/TiO_2$	Pyrex Glass	84%/500nm	Rf Sputtering techniques	[50]
$TiO_2/Au/TiO_2$	Polymer	Over 80%/680nm	Magnetron sputtering	[51]
$Al_2O_3/Ag/Al_2O_3$	Silicon solar cell	88%/330nm	Physical vapour deposition	[52]
ZnS/Ag/ZnS	Glass	80%/550nm	Thermal evaporation	[28]
ZnO/Ag/ZnO	Flexible PET	88%/550nm	Magnetron sputtering	[53]

Table 2. The optical properties of different samples. Tp represents the peak of visible transmittance.

Structure	Thickness(nm)	Visible Transmittance	Solar Infrared Reflectance	Reference
ZnO/Ag/ZnO	42.7/12.7/39.7	T_{vis}=87.1% T_p=88%	R_{si}=58.9% R_λ=1900=86.7%	[28]
ZnO/Ag/ZnO	37.7/17.9/35.7	T_{vis}=76.4% T_p=84.3%	R_{si}=78.6% R_λ=1900=93.4%	[28]
ZnS/Ag/ZnS	37/21/37	T_{vis}=83.9%	R_λ=1900 - 91%	[54]
ZnS/Ag/ZnS	31/20/34	T_p - 80%	R_λ=1900 - 91%	[55]
$TiO_2/Ag/TiO_2$	18/18/18	T_p=84%	R_λ=1900 - 92%	[50]
$TiO_2/Ag/TiO_2$	33/20/33	T_p - 76 %	R_λ=1900 - 89%	[55]
$TiO_2/Ag/TiO_2$	48/18/48	T_{vis}=62.5%	R_{si} - 71.9%	[56]
$TiO_2/cu/TiO_2$	50/20/50	T_{vis}=59.8%	R_{si} - 85.6%	[56]
$WO_3/Ag/WO_3$	37/20/37	T_p - 82%	R_λ=1900 - 89%	[55]
$WO_3/Ag/WO_3$	25/16/25	T_{vis}=74% T_p=77%	R_{si}=57.2% R_λ=1900=80%	[57]

In the Past multilayer dielectric/metal/dielectric (D/M/D) structures have been explored for optimizing optical and electrical properties. ZnO/Ag/ZnO films were designed to utilize plasmonic effects [58] with ZnO layers (30-40 nm) and Ag (6 nm), achieving high transparency and a Wurtzite structure at 300°C. $WO_3/Au/WO_3$ multilayers, fabricated via thermal evaporation, showed optimal transmittance (84%) with a 36 nm Au layer [49]. Similarly, WO3/Ag/WO3 coatings with Ag thickness ≥18 nm exhibited enhanced visible transmittance (88.3%) and heat mirror behavior [55].

ZnO/Ag/ZnO films on PET, deposited via DC magnetron sputtering, demonstrated tunable optical and electrical properties [53]. Their application as IR reflective coatings resulted in 9.6% cooling energy savings [28]. NiO/Ag/NiO (NAN) films exhibited high transmittance (82%) and improved power conversion efficiency in organic PVs [59]. TiO2/Ag/TiO2 coatings demonstrated 84% visible transmittance and 98-99% IR reflectivity, promising for solar-thermal applications [50].

TiO2/Au/TiO2 multilayers on polymers optimized transmittance (>80%) by tuning TiO2 and Au thickness [51]. A four-layer waveguide structure incorporating Ag-Au nanoparticles enhanced solar cell efficiency through controlled reflection and transmission [40]. SiO2/ZnO/TiO2 triple layers minimized reflections and maximized transmittance when a high-index ZnO layer was sandwiched between two low-index materials [60].

3.1 D/M/D material deposition techniques

The optical properties of D/M/D films are directly related to the exact chemistry and physical morphology of the coatings. Oxide coatings depend upon stoichiometry, impurities, and defects in films while metal films are dependent on nucleation and coalescence phenomena. In all films, crystal structure and impurities influence both electrical and optical conductivity [33]. Due to the above correlations, various deposition techniques or even alterations of fixed techniques can result in a vast range of film properties. Deposition techniques, high substrate temperature or electron/ion influence, and alkali element diffusion can lead to serious problems. Also, high temperatures can induce diffusion between layers and the reaction of alkaline ions under certain conditions. Typically, plastic substrates are limited to 100-250°C temperature heating, and at high temperatures, plastic can melt or soften or thermally expand. Even though many plastics are prone to oxidation, decomposition, or reduction, which can decrease their strength [33].

Therefore, the selection of deposition technique according to substrate properties is essential. The various deposition techniques used for layer deposition over solar cells can be introduced as chemical vapour deposition (CVD) technique, evaporative physical vapour deposition (PVD; vapor plating), magnetron sputtering, electron beam deposition, ion beam plating (plasma-assisted process), and atomic layer deposition [61] as shown below in Figure 14.

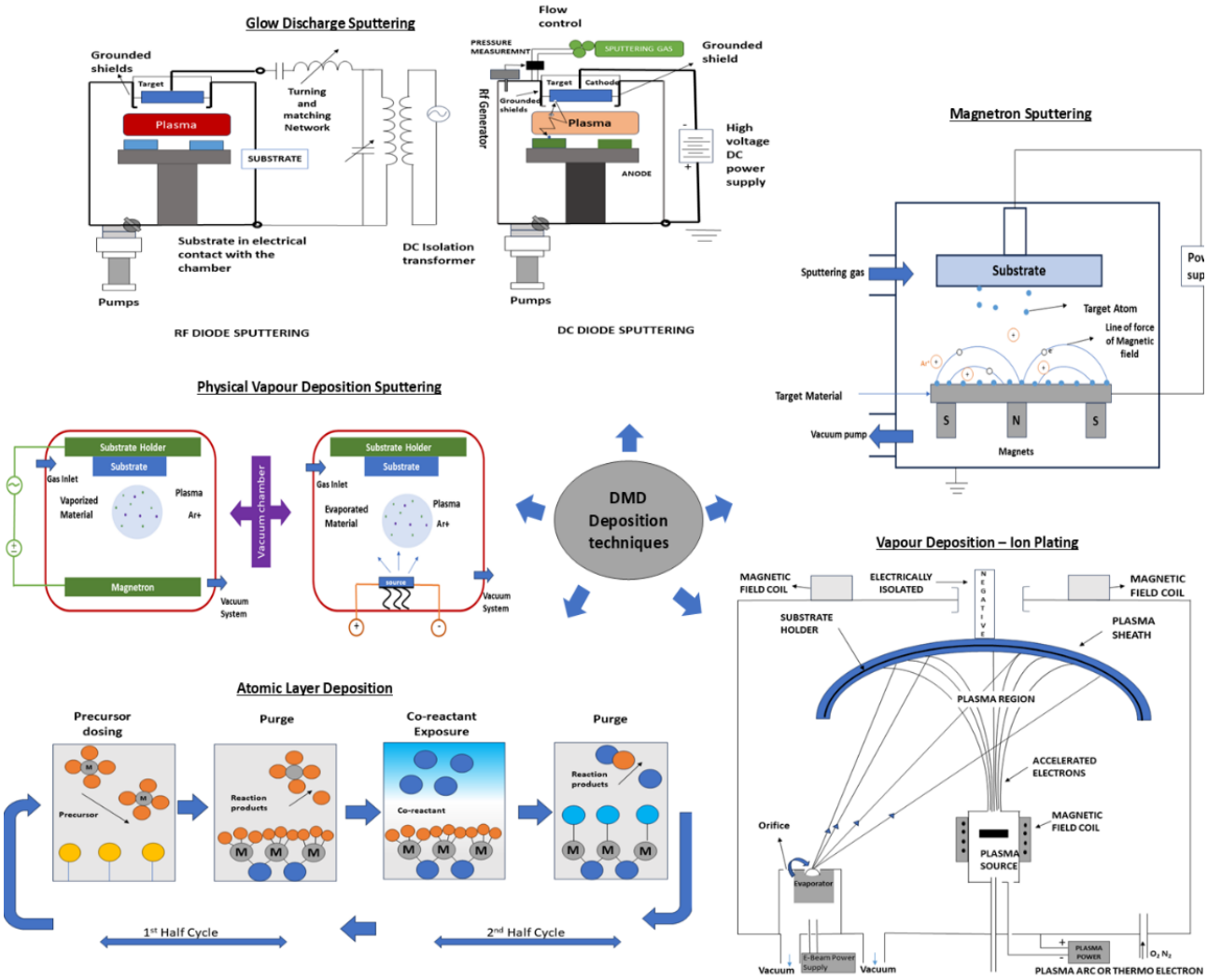

Fig. 14 Systematic layout of various techniques used for DMD deposition. [47-49, 61-71]. The above techniques are used to fabricate multilayer optical filters of different thicknesses on a given substrate to optimize the transmittance or reflectance for particular wavelengths (Adapted with permission from Publisher)

4. FACTORS AFFECTING TRANSMITTANCE AND REFLECTANCE SPECTRA OF DMD LAYER

4.1 Effect of D/M/D layer thickness on transmittance and reflectance using different substrates

Numerous studies have analyzed the impact of D/M/D layer thickness on optical properties. Reflectance and transmittance are key considerations in film design, with optimization tools employed to determine ideal layer thickness. Researchers have proposed various methods for optimization.

For instance, [28] experimentally investigated ZnO/Ag/ZnO structures, varying Ag layer thickness from 12 nm to 50 nm. Using ray tracing methods, it was observed that long-wave emittance (εlw) decreased from 5% to 1.3% as Ag thickness increased, indicating low emittance for continuous Ag layers. Visible transmittance (Tvis) and solar infrared reflectance (Rsi) were evaluated for varying Ag thickness, as shown in Figure 15.

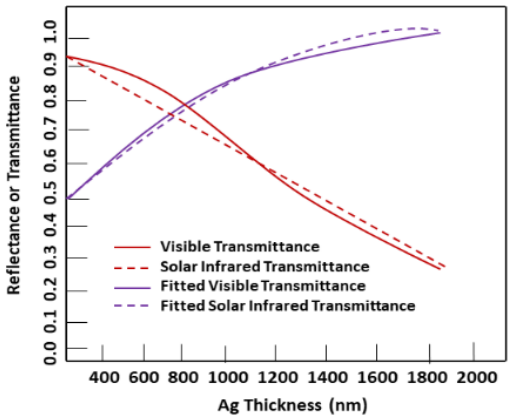

Fig. 15. Solar infrared reflectance and the fitted ones with Ag thickness varying from 12 nm to 50 nm [9] (Adapted with permission from Publisher).

The fitted functions of T_{vis} and R_{si} with the thickness t (nm) for Ag are obtained; T_{vis} =1.105-0.02 x^2 and R_{si}= 0.412 + 0.151x ln (t-10.191) i.e., a linear decreasing function for R_{si}. The adjusted R-squares of the two functions are 99.02 % and 99.5 %, respectively, indicating the two functions are well fitted. For magnetron sputtering, a continuous Ag layer requires a minimum thickness of 12 nm, with T_{vis} dropping below 15% at 50 nm. The optimal Ag thickness of 17.7 nm achieves T_{vis} = 0.751 and R_{si} = 0.716, offering a balance for ZnO/Ag/ZnO/PET applications. A study [50] on TiO_2/Ag/TiO_2 multilayers shown in Fig. 16(b) found that a 180 Å Ag layer sandwiched between TiO_2 layers yielded the best results, with an optimum TiO_2 thickness of 180 Å for maximum transmittance at 0.5 µm, where the outer TiO_2 layer acts as protection and the inner layer binds Ag to the substrate. For WO_3/Au/WO_3 heat mirrors [45], gold layers < 20 nm lacked selectivity, while layers >20 nm confined transmittance to the visible range, increased infrared reflectance, and shifted the peak transmittance to higher wavelengths. The dielectric layer enhanced transmittance via antireflection, with reflectance negligible below 600 nm, is depicted in Figure16.

Similarly, the authors [49] estimated the performance of WO3/Ag/WO3 transparent heat mirrors as shown in Fig.17 for different thicknesses of the silver layer. The WO3 thickness was fixed 35 nm. Detailed analysis, based on complex optical admittance, has shown that the thickness of the dielectric layer must be greater than λ/8 nd, where nd is the dielectric refractive index. For our case nd = 2.014 at λ = 550nm, the minimum thickness of the dielectric should be 34 nm. The thickness of the silver layer plays an important role in deciding the operation of the heat mirror. The heated mirror with a very thin layer of film did not exhibit the required selectivity. For thickness > 24 nm, the selectivity was improved. The following observation can be made:

1. Transmittance was confined to the visible range
2. As the silver layer's thickness increased, the transmittance bandwidth narrowed.
3. As the thickness of the silver layer increased, the maximum transmittance increased as well as infrared reflectance progressively increased.
4. The minimum reflectance was found around 550 nm wavelength and the wavelength shifted to lower values as the thickness of the silver layer increased.

A study [54] on ZnS/Ag/ZnS films found that increasing Ag thickness reduces transmittance. A 100Å Ag layer achieves ~93% Tlum but faces fabrication challenges since Ag films below 120-150Å tend to be granular [10, 72, 73]. A more practical Ag thickness of 150-200Å yields Tlum of 92.5% and 84%, respectively, with high IR reflectance. The ZnS layer thickness has minimal impact on IR reflectivity, increasing it by only 2.5%, and allowing transmission optimization.

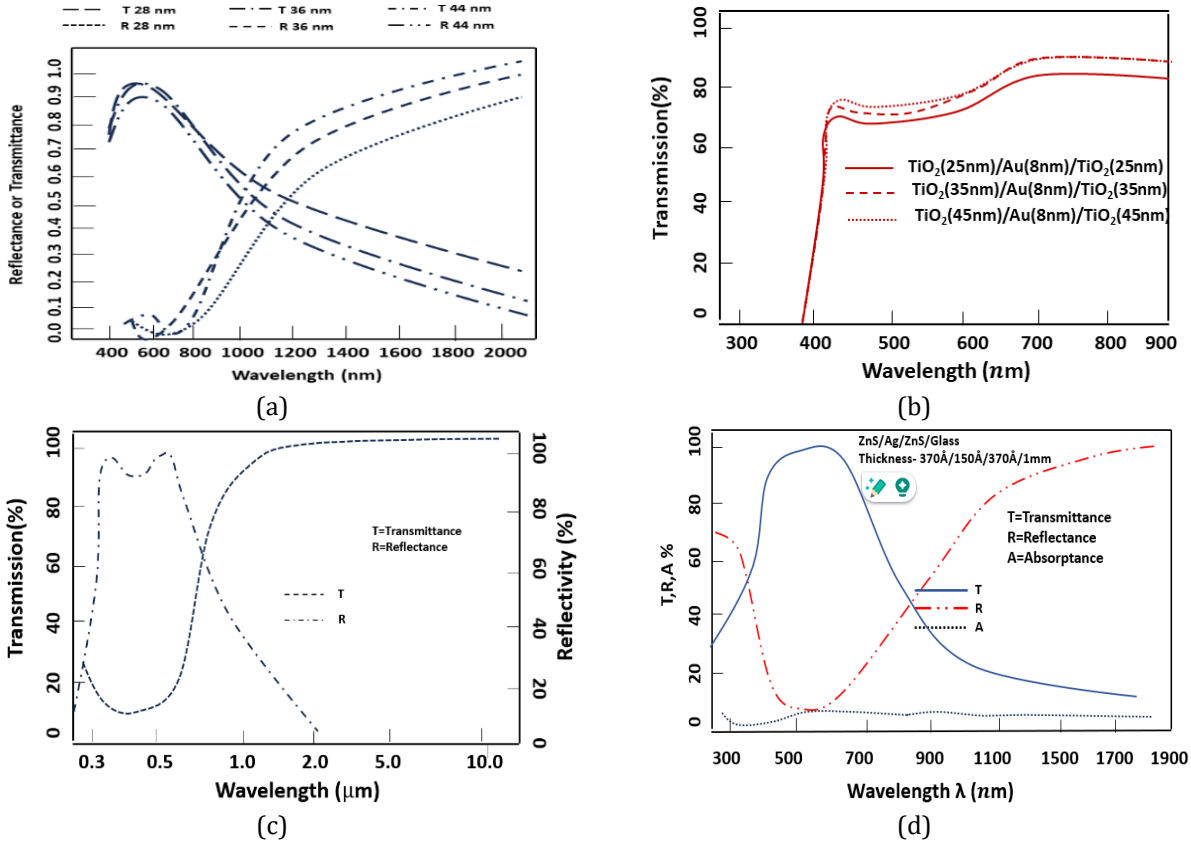

Fig. 16 Transmittance and reflectance spectra of (a) $WO_3/Au/WO_3$ (b) $TiO_2/Ag/TiO_2$ (c) $TiO_2/Au/TiO_2$ (d) ZnS/Ag/ZnS [49, 53, 74-76](Adapted with permission from Publisher).

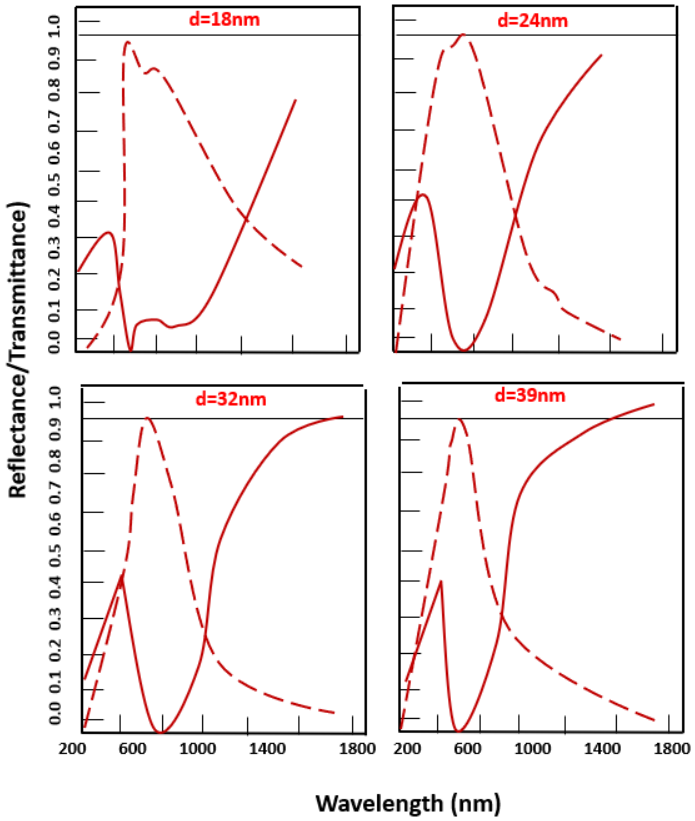

Fig. 17. Reflectance (R) and transmittance (T) spectra of the heat mirrors ($WO_3/Ag/WO_3$/glass. The thickness of WO_3 was kept at 35 nm. The thickness of the silver film is indicated in the figures. For comparison, the dashed line shows the 90 % value of either quantity [45]. Adapted with permission from the publisher.

For TiO2/Au/TiO2 films on polymers [51], TiO2 enhances visible transmittance, with the outer layer serving as a protective coating and the inner layer aiding adhesion. Increasing Au thickness beyond 8 nm reduces transmittance while increasing reflectance. At 680 nm, transmittance exceeds 80%, with an average of 80% across the visible spectrum. Optimized transmittance occurs at 8 nm Au and 45 nm TiO2 layers, as shown in Figure 16.

In Fig. 18a, the transmittance is plotted as a function of the thickness of the top dielectric layer(d3) and bottom dielectric layer (d1), where f=d3/d1 and for different value of f, different plot has been shown in Fig. 18a. The maximum transmittance is for f=1, which means for maximum transmittance the value of thickness for top and bottom dielectric should be same.

Similarly, using data of Fig 18a, the maximum transmittance was plotted as a function of refractive index in Fig 18b, which shows that for the maximum value of transmittance, we require a high refractive index in the visible region for a dielectric material of thickness d1. Once the dielectric is selected, Fig. 18a can be used for the design of the D/M/D structure for optimum performance. As shown in Fig 19, the variation of measured spectral reflectance and transmittance for different D/M/D structures on a glass substrate has been illustrated. It shows the structure of WO3/Ag/WO3/glass, ZnS/Ag/ZnS/glass, and TiO2/Ag/TiO2/unheated glass, where an average transmittance of 0.7 in the visible region is observed. But in the case of heated glass, the average transmittance is just 0.4, which may be due to interdiffusion of material at different interfaces.

4.2 Effect of refractive index (n) and absorption coefficient (k) of D/M/D layer on transmittance and reflectance

Most films rely on high and low refractive index layers, utilizing refractive index differences and layer thickness for optical performance [47]. A D/M/D film was designed and fabricated on glass [77] as a spectrally selective filter [60, 54, 74, 78-81], reflecting IR while transmitting visible light. The metal layer, which typically transmits little visible energy, was sandwiched between dielectric layers acting as antireflection coatings to enhance transmission.

Optimization focused on maximizing visible transmittance while controlling IR reflectance. Using Heaven's matrix formulation [27], a systematic study analyzed the effect of each layer, modeled as air/D(n1, k1)/M(n2, k2)/D(n3, k3)/glass(n4, k4), with negligible absorption ($k \approx 0$). Since n1 = n3, identical dielectric materials were assumed. Transmittance measured in the air was ~4% lower than in glass, with further details in subsequent discussions.

Table 3. Refractive index (n) and absorption Index (k; only for Ag) at different wavelengths (λ) [82].

λ(nm)	Ag(n)	Ag(k)	TiO_2(n)	WO_3(n)	TiO_2(n) (at 300°C)	ZnS(n)
2000	0.25	14.50	1.94	1.79	2.10	2.23
1900	0.22	13.75	1.94	1.79	2.10	2.23
1800	0.20	13.15	1.95	1.80	2.10	2.24
1700	0.18	12.50	1.95	1.80	2.11	2.24
1600	0.16	11.80	1.96	1.80	2.11	2.25
1500	0.14	11.03	1.96	1.81	2.12	2.25
1400	0.12	10.10	1.97	1.81	2.12	2.26
1300	0.10	9.50	1.97	1.82	2.13	2.26
1200	0.09	8.70	1.98	1.82	2.13	2.27
1100	0.07	8.00	1.99	1.83	2.14	2.28
1000	0.06	7.18	1.99	1.83	2.14	2.29
900	0.06	6.40	2.00	1.84	2.15	2.30
800	0.05	5.60	2.00	1.85	2.16	2.32
700	0.05	4.80	2.01	1.87	2.18	2.33
600	0.05	4.00	2.02	1.89	2.21	2.35
500	0.05	3.07	2.04	1.93	2.27	2.39
400	0.05	2.25	2.05	2.05	2.40	2.56

From Table 3, it can be inferred that Ag acts as a lossy metallic layer and TiO_2 / WO_3 / ZnS acts as phase-controlling dielectric layers, which is perfect for designing DMD (Dielectric–Metal–Dielectric) coatings and FP resonators for selective absorption or cooling applications.

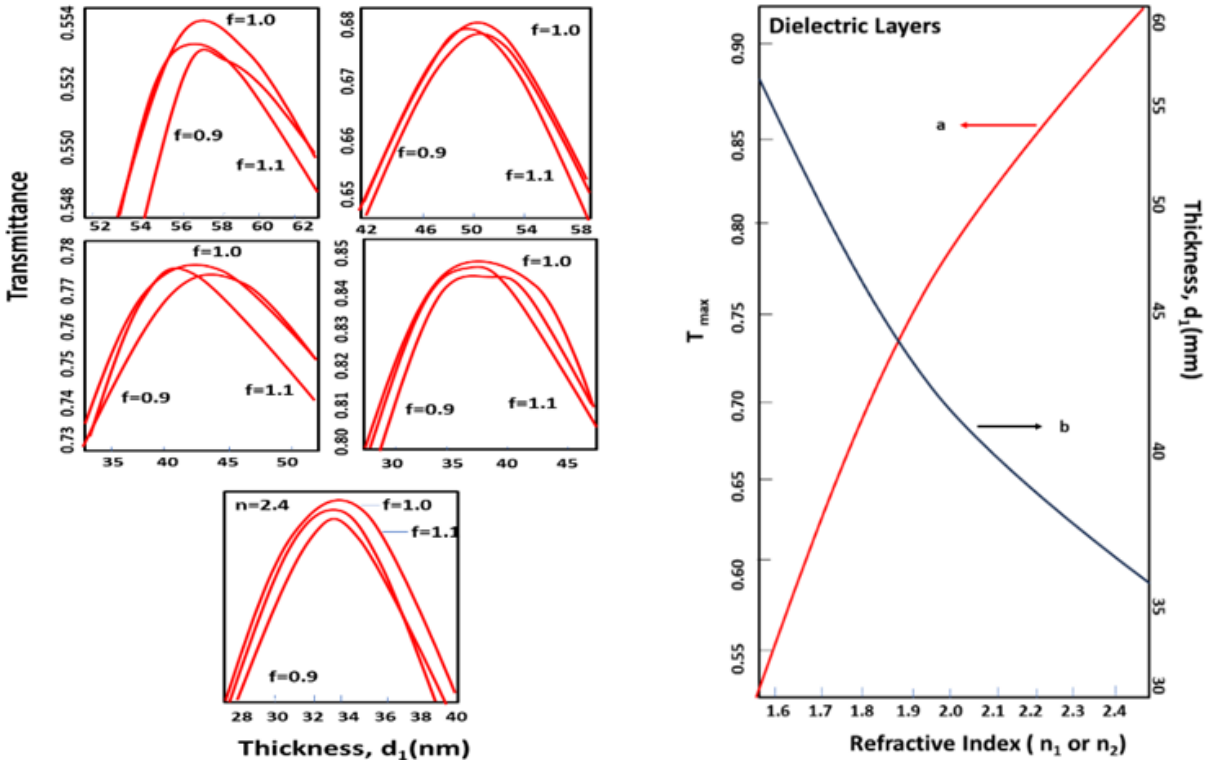

Fig. 18. (a) Computer simulations for optimization of D/M/D layers on a glass system. The two D-layers in the system are of the same dielectric. Effects of a thickness (d_1 and d_3) of dielectric layers on transmittance at a wavelength of 550 nm for different values of f (=d_3/d_1) are shown for dielectrics with refractive indices of (a) 1.6 (b) 1.8 (c) 2.0 (d) 2.2 and (e) 2.4 (b) Dependences of (1) maximum value of the transmittance and (2) thickness of the dielectric layer(s) on the refractive index of a dielectric are shown [77]. Adapted with permission from the publisher.

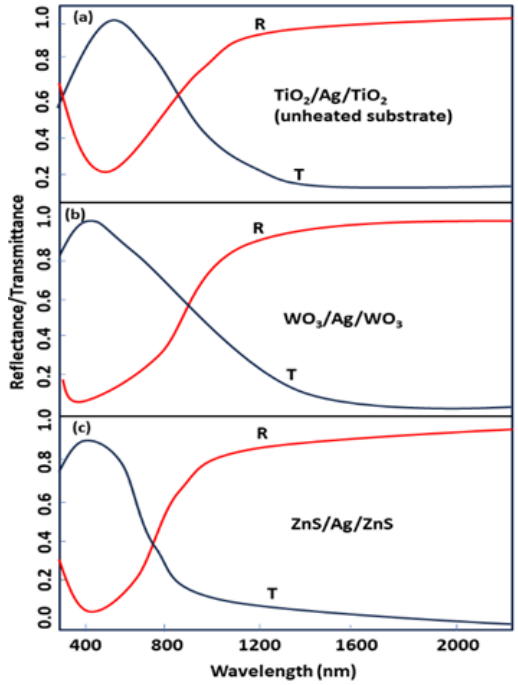

Fig. 19. Measured reflectance and transmittance of D/M/D on glass systems for the different dielectrics [77]. Adapted with permission from Publisher.

5. CHALLENGES

The passive cooling of solar cells using spectrally selective Dielectric/Metal/Dielectric (D/M/D) filters has garnered significant interest, particularly for flexible solar cells in portable electronics and defence applications. However, future research is required in nanomaterial engineering and deposition techniques to enable the integration of these coatings onto flexible substrates, as most existing studies primarily focus on rigid materials such as glass and quartz. A key challenge is the limited research on D/M/D films for flexible substrates, which raises uncertainties regarding their real-world applicability. While D/M/D coatings enhance solar cell efficiency, they should be integrated into the cell structure rather than externally applied, and their long-term stability must be evaluated under environmental stressors such as humidity, UV exposure, and temperature fluctuations [83-88]. Additionally, flexible substrates such as

polyethylene terephthalate (PET) and polyethylene naphthalate (PEN) have low thermal stability, necessitating the use of compatible deposition techniques like atomic layer deposition (ALD). Furthermore, large-scale and cost-effective manufacturing of D/M/D filters remains a challenge due to the high cost of dielectric materials and deposition processes. Although spectrally selective passive cooling effectively reduces solar cell temperature and improves efficiency, it is crucial to ensure that these filters do not compromise the absorption of solar cells, as excessive optical losses could counteract the benefits of thermal regulation [18].

6. OUTLOOK

To enable seamless integration of these coatings onto flexible substrates, future research should focus on developing low-temperature compatible nanomaterials and deposition techniques. Dielectric materials such as Al_2O_3, TiO_2, and SiO_2, along with ultrathin metal layers like Ag or Al, can be deposited using atomic layer deposition (ALD), which offers excellent uniformity and precision at low processing temperatures suitable for polymers like polyethylene terephthalate (PET) and polyethylene naphthalate (PEN) [89-92]. Nanostructured dielectric films, including nanolaminates or nanocomposites, can be engineered to tailor optical properties while maintaining mechanical flexibility and strong adhesion to flexible substrates.

To accommodate large-scale production, scalable methods such as spatial ALD, low-temperature sputtering, and solution-based processes like sol–gel or inkjet printing should be optimized for roll-to-roll (R2R) manufacturing [93]. Integration of D/M/D filters directly into the solar cell structure, rather than as externally applied layers, ensures better durability and optical efficiency [90]. Co-designing the D/M/D coatings as part of the encapsulation layer or combining them with transparent conductive oxides can enhance functionality without compromising transparency in the active spectral region.

Optical modeling using techniques such as finite-difference time-domain (FDTD) simulations is essential to design coatings that reflect unwanted infrared radiation while maximizing transmission in the visible and near-infrared regions critical for photovoltaic conversion [89]. Environmental stability can be achieved by incorporating UV-resistant barrier layers and hybrid encapsulation techniques that offer high resistance to moisture and oxygen ingress. Accelerated aging tests under controlled UV, temperature, and humidity conditions should be conducted to assess long-term reliability [94-96]. To reduce costs, material efficiency can be improved by minimizing layer thickness and using cost-effective alternatives for metals and dielectrics. Incorporating real-time monitoring and machine learning algorithms into R2R manufacturing lines can further enhance process control and yield. Pilot-scale flexible solar cell prototypes with embedded D/M/D filters should be developed and tested under realistic operating conditions to validate thermal performance, mechanical integrity, and overall efficiency gains. With these innovations, D/M/D coatings can be effectively transitioned from rigid substrates to high-performance flexible solar cells, enabling reliable, thermally managed photovoltaics for next-generation portable and wearable energy systems.

7. CONCLUSIONS

This study reviewed passive cooling techniques for flexible solar cells using spectrally selective Dielectric/Metal/Dielectric (D/M/D) filters, which selectively filter unwanted photons while transmitting effective ones for electron-hole pair creation. The findings highlight that D/M/D filters significantly reduce the operating temperature of flexible solar cells, with their optical performance primarily governed by layer thickness, refractive index, and absorption coefficient. Dielectric materials such as TiO2, WO3, and ZnS exhibit minimal absorption in the 400–2000 nm range, making refractive index engineering crucial for optimizing transmittance and reflectance. Among the studied configurations, ZnS/Ag/ZnS achieved the highest visible transmittance (T_{vis} = 83.9%) and infrared reflectance ($R_\lambda \approx 91\%$), whereas TiO_2/Cu/TiO_2 exhibited the lowest T_{vis} at 59.8%. Given the temperature sensitivity of flexible substrates such as PET, PEN, and polyimides, low-temperature deposition techniques like atomic layer deposition (ALD) are preferred for maintaining substrate integrity. Material selection and deposition methods play a critical role in ensuring the large-scale integration of D/M/D coatings with flexible solar cells. To enable passive cooling, an ideal D/M/D film should possess high visible transmittance (380–780 nm) and strong

infrared reflectance (780–2500 nm), with the metal layer serving as an IR reflector while dielectric layers provide surface passivation. Silver remains the preferred metal due to its minimal optical losses. Future research should focus on optimizing D/M/D coatings for flexible substrates and developing scalable fabrication techniques to facilitate commercial adoption.

Author contributions

The Corresponding Author (Main Author) and Co-Author conceptualized the review framework, conducted the literature survey, analyzed the collected data, and drafted the manuscript, while the other Author provided critical revisions and supervised the study.

REFERENCES

[1] International Energy Agency (IEA), *Renewables 2027: Analysis and Forecasts to 2027*. Available: https://www.iea.org, accessed Jan. 1, 2026.

[2] M. Pagliaro, R. Ciriminna, and G. Palmisano, "Flexible solar cells," *ChemSusChem*, vol. 1, no. 11, pp. 880–891, Oct. 2008, doi: 10.1002/cssc.200800127.

[3] International Energy Agency (IEA), *Renewables 2025: Analysis and Forecast to 2025*. Available: https://www.iea.org, accessed Jan. 1, 2026.

[4] T. D. Lee and A. U. Ebong, "A review of thin film solar cell technologies and challenges," *Renewable and Sustainable Energy Reviews*, vol. 70, pp. 1286–1297, Dec. 2016, doi: 10.1016/j.rser.2016.12.028.

[5] D. C. Olson and D. S. Ginley, "Nanostructured TCOs (ZnO, TiO2, and Beyond)," in *Handbook of Transparent conductors*, 2010, pp. 425–457. doi: 10.1007/978-1-4419-1638-9_12.

[6] S. Kim, H. Van Quy, and C. W. Bark, "Photovoltaic technologies for flexible solar cells: beyond silicon," *Materials Today Energy*, vol. 19, p. 100583, Nov. 2020, doi: 10.1016/j.mtener.2020.100583.

[7] X. Li, P. Li, Z. Wu, D. Luo, H.-Y. Yu, and Z.-H. Lu, "Review and perspective of materials for flexible solar cells," *Materials Reports Energy*, vol. 1, no. 1, p. 100001, Dec. 2020, doi: 10.1016/j.matre.2020.09.001.

[8] B. R. Paudyal and A. G. Imenes, "Investigation of temperature coefficients of PV modules through field measured data," *Solar Energy*, vol. 224, pp. 425–439, Jun. 2021, doi: 10.1016/j.solener.2021.06.013.

[9] S. Dang, Y. Yi, and H. Ye, "A visible transparent solar infrared reflecting film with a low long-wave emittance," *Solar Energy*, vol. 195, pp. 483–490, Dec. 2019, doi: 10.1016/j.solener.2019.11.080.

[10] Y. An, C. Sheng, and X. Li, "Radiative cooling of solar cells: opto-electro-thermal physics and modeling," *Nanoscale*, vol. 11, no. 36, pp. 17073–17083, Jan. 2019, doi: 10.1039/c9nr04110a.

[11] K. A. Moharram, Abd-Elhady, H. A. Kandil, and H. El-Sherif, "Enhancing the performance of photovoltaic panels by water cooling," *Ain Shams Engineering Journal*, vol. 4, no. 4, pp. 869–877, May 2013, doi: 10.1016/j.asej.2013.03.005.

[12] S. Chander, A. Purohit, A. Sharma, S. P. Nehra, and Dhaka, "Impact of temperature on performance of series and parallel connected mono-crystalline silicon solar cells," *Energy Reports*, vol. 1, pp. 175–180, Sep. 2015, doi: 10.1016/j.egyr.2015.09.001

[13] T. Dewi, A. Taqwa, C. Sitompul, R. Kusumanto, and Rusdianasari, "Active and passive cooling comparison of PV panels applied in Tropical City: case study Palembang, South Sumatra," I*OP Conference Series Earth and Environmental Science*, vol. 709, no. 1, p. 012005, Mar. 2021, doi: 10.1088/1755-1315/709/1/012005.

[14] P. Dwivedi, K. Sudhakar, A. Soni, E. Solomin, and I. Kirpichnikova, "Advanced cooling techniques of P.V. modules: A state of art," *Case Studies in Thermal Engineering*, vol. 21, p. 100674, Jun. 2020, doi: 10.1016/j.csite.2020.100674.

[15] S. A. Nada and D. H. El-Nagar, "Possibility of using PCMs in temperature control and performance enhancements of free stand and building integrated PV modules," *Renewable Energy*, vol. 127, pp. 630–641, May 2018, doi: 10.1016/j.renene.2018.05.010.

[16] A. S. S. Bilal et al., "PCM-integrated windows for enhanced passive cooling: an experimental and numerical investigation," *Heat and Mass Transfer*, vol. 61, no. 4, Mar. 2025, doi: 10.1007/s00231-025-03549-5.

[17] M. Sharaf, M. S. Yousef, and A. S. Huzayyin, "Review of cooling techniques used to enhance the efficiency of photovoltaic power systems," *Environmental Science and Pollution Research*, vol. 29, no. 18, pp. 26131–26159, Jan. 2022, doi: 10.1007/s11356-022-18719-9.

[18] Y. An, C. Sheng, and X. Li, "Radiative cooling of solar cells: opto-electro-thermal physics and modeling," *Nanoscale*, vol. 11, no. 36, pp. 17073–17083, Jan. 2019, doi: 10.1039/c9nr04110a.

[19] Z. Wu et al., "A review of spectral controlling for renewable energy harvesting and conserving," *Materials Today Physics*, vol. 18, p. 100388, Mar. 2021, doi: 10.1016/j.mtphys.2021.100388.

[20] H. Watanabe, J. Ishii, H. Wakabayashi, T. Kumano, and L. Hanssen, "Spectral emissivity measurements," in *Experimental methods in the physical sciences*, 2014, pp. 333–366. doi: 10.1016/b978-0-12-386022-4.00009-1.

[21] M. Diab and O. Alabbosh, "Title unavailable," *Advances in Physics Theories and Applications*, vol. 70, p. 27, 2018.

[22] U. Banik et al., "Enhancing passive radiative cooling properties of flexible CIGS solar cells for space applications using single layer silicon oxycarbonitride films," *Solar Energy Materials and Solar Cells*, vol. 209, p. 110456, Feb. 2020, doi: 10.1016/j.solmat.2020.110456.

[23] L. Zhu, A. Raman, K. X. Wang, M. A. Anoma, and S. Fan, "Radiative cooling of solar cells," *Optica*, vol. 1, no. 1, p. 32, Jul. 2014, doi: 10.1364/optica.1.000032.

[24] W. Li, Y. Shi, K. Chen, L. Zhu, and S. Fan, "A comprehensive photonic approach for solar cell cooling," *ACS Photonics*, vol. 4, no. 4, pp. 774–782, Mar. 2017, doi: 10.1021/acsphotonics.7b00089.

[25] G. Perrakis, A. C. Tasolamprou, G. Kenanakis, E. N. Economou, S. Tzortzakis, and M. Kafesaki, "Passive radiative cooling and other photonic approaches for the temperature control of photovoltaics: a comparative study for crystalline silicon-based architectures," *Optics Express*, vol. 28, no. 13, p. 18548, Mar. 2020, doi: 10.1364/oe.388208.

[26] J. Kischkat et al., "Mid-infrared optical properties of thin films of aluminum oxide, titanium dioxide, silicon dioxide, aluminum nitride, and silicon nitride," *Applied Optics*, vol. 51, no. 28, p. 6789, Sep. 2012, doi: 10.1364/ao.51.006789.

[27] O.S Heavens, *Optical properties of thin solid films*,1st edition. New York: Dover Publications,1991.

[28] S. Dang, Y. Yi, and H. Ye, "A visible transparent solar infrared reflecting film with a low long-wave emittance," *Solar Energy*, vol. 195, pp. 483–490, Dec. 2019, doi: 10.1016/j.solener.2019.11.080.

[29] M. Nur-E-Alam, M. Vasiliev and K. Alameh, "Dielectric/metal/dielectric (DMD) multilayers: Growth and stability of ultra-thin metal layers for transparent heat regulation (THR)." In *Energy Saving Coating Materials*, pp. 83-112. Elsevier, 2020. doi: 10.1016/B978-0-12-822103-7.00004-2

[30] B. Zhao, M. Hu, X. Ao, Q. Xuan, and G. Pei, "Spectrally selective approaches for passive cooling of solar cells: A review," *Applied Energy*, vol. 262, p. 114548, Jan. 2020, doi: 10.1016/j.apenergy.2020.114548.

[31] X. Sun, T. J. Silverman, Z. Zhou, M. R. Khan, P. Bermel, and M. A. Alam, "Optics-Based approach to thermal management of photovoltaics: Selective-Spectral and radiative cooling," *IEEE Journal of Photovoltaics*, vol. 7, no. 2, pp. 566–574, Jan. 2017, doi: 10.1109/jphotov.2016.2646062.

[32] B. Karlsson, E. Valkonen, T. Karlsson, and C. -g. Ribbing, "Materials for solar-transmitting heat-reflecting coatings," *Thin Solid Films*, vol. 86, no. 1, pp. 91–98, Nov. 1981, doi: 10.1016/0040-6090(81)90162-0.

[33] C. M. Lampert, "Heat mirror coatings for energy conserving windows," *Solar Energy Materials*, vol. 6, no. 1, pp. 1–41, Nov. 1981, doi: 10.1016/0165-1633(81)90047-2.

[34] S. Suman, Mohd. K. Khan, and M. Pathak, "Performance enhancement of solar collectors—A review," *Renewable and Sustainable Energy Reviews*, vol. 49, pp. 192–210, May 2015, doi: 10.1016/j.rser.2015.04.087

[35] H.S. Nalwa, *Handbook of thin films*,1st edition. United States: Academic Press, 2001.

[36] N. Venugopal and A. Mitra, "Optical transparency of ZnO thin film using localized surface plasmons of Ag nanoislands," *Optical Materials*, vol. 35, no. 7, pp. 1467–1476, Mar. 2013, doi: 10.1016/j.optmat.2013.03.003.

[37] H.-Y. Pan, X. Chen, and X.-L. Xia, "A review on the evolvement of optical-frequency filtering in photonic devices in 2016–2021," *Renewable and Sustainable Energy Reviews*, vol. 161, p. 112361, Mar. 2022, doi: 10.1016/j.rser.2022.112361.

[38] Q. Li et al., "Tunable perfect Narrow-Band absorber based on a Metal-Dielectric-Metal structure," *Coatings*, vol. 9, no. 6, p. 393, Jun. 2019, doi: 10.3390/coatings9060393.

[39] A. Bahrami, S. Mohammadnejad, N.J. Abkenar, and S. Soleimaninezhad, "Optimized single and double layer antireflection coatings for GaAs solar cells." *International journal of renewable energy research* vol. 3, no. 1, pp 79-83, 2013.

[40] F. Demichelis, E. Minetti-Mezzetti, and V. Perotto, "Optical studies of multilayer dielectric-metal-dielectric coatings as applied to solar cells," *Solar Cells*, vol. 6, no. 4, pp. 323–333, Sep. 1982, doi: 10.1016/0379-6787(82)90071-0.

[41] G. K. Dalapati et al., "Transparent heat regulating (THR) materials and coatings for energy saving window applications: Impact of materials design, micro-structural, and interface quality on the THR performance," *Progress in Materials Science*, vol. 95, pp. 42–131, Feb. 2018, doi: 10.1016/j.pmatsci.2018.02.007.

[42] M. Nur-E-Alam, M.D. Momtazur, M.D. Rahman, B.M. Khairul, M. Vasiliev and K. Alameh "Optical and chromaticity properties of metal-dielectric composite-based multilayer thin-film structures prepared by RF magnetron sputtering", *Coatings*, 10(3), p.251

[43] M. F. Al-Kuhaili, A. H. Al-Aswad, S. M. A. Durrani, and I. A. Bakhtiari, "Energy-saving transparent heat mirrors based on tungsten oxide–gold WO3/Au/WO3 multilayer structures," *Solar Energy*, vol. 86, no. 11, pp. 3183–3189, Sep. 2012, doi: 10.1016/j.solener.2012.08.008.

[44] L. Zhu, A. Raman, K. X. Wang, M. A. Anoma, and S. Fan, "Radiative cooling of solar cells," *Optica*, vol. 1, no. 1, p. 32, Jul. 2014, doi: 10.1364/optica.1.000032.

[45] J. H. Kim et al., "Highly flexible Al-doped ZnO/Ag/Al-doped ZnO multilayer films deposited on PET substrates at room temperature," *Ceramics International*, vol. 42, no. 2, pp. 3473–3478, Nov. 2015, doi: 10.1016/j.ceramint.2015.10.146.

[46] J. Leng et al., "Influence of Ag thickness on structural, optical, and electrical properties of ZnS/Ag/ZnS multilayers prepared by ion beam assisted deposition," *Journal of Applied Physics*, vol. 108, no. 7, Oct. 2010, doi: 10.1063/1.3490787.

[47] C. Wang, J. Wang, J. Wang, H. Du, and J. Wang, "Optimal design and analysis of refractive index and thickness gradient optical films," *Results in Optics*, vol. 5, p. 100161, Oct. 2021, doi: 10.1016/j.rio.2021.100161.

[48] V. Zardetto et al., "Atomic layer deposition for perovskite solar cells: research status, opportunities and challenges," *Sustainable Energy & Fuels*, vol. 1, no. 1, pp. 30–55, Jan. 2017, doi: 10.1039/c6se00076b.

[49] M. F. Al-Kuhaili, A. H. Al-Aswad, S. M. A. Durrani, and I. A. Bakhtiari, "Transparent heat mirrors based on tungsten oxide–silver multilayer structures," *Solar Energy*, vol. 83, no. 9, pp. 1571–1577, Jun. 2009, doi: 10.1016/j.solener.2009.05.006

[50]. H. Y. Fan and C. C. Lee, "Two-photon absorption with exciton effect for degenerate valence bands," P*hysical Review. B, Solid State*, vol. 9, no. 8, pp. 3502–3516, Apr. 1974, doi: 10.1103/physrevb.9.3502.

[51] J. Zhou, Z. Wu, and Z. Liu, "Optical and electrical properties of TiO2/Au/TiO2 multilayer coatings in large area deposition at room temperature," *Rare Metals*, vol. 27, no. 5, pp. 457–462, Oct. 2008, doi: 10.1016/s1001-0521(08)60162-x.

[52] S. Li, Y. Dan, J. Zhou, and H. Shen, "Al2O3/Ag/Al2O3 passivating and conducting stacks for crystalline silicon solar cells," *Thin Solid Films*, vol. 615, pp. 56–62, Jul. 2016, doi: 10.1016/j.tsf.2016.07.002.

[53] X. Yu, D. Zhang, P. Wang, R.-I. Murakami, B. Ding, and X. Song, "The optical and electrical properties of ZnO/Ag/ZnO films on flexible substrate," *International Journal of Modern Physics Conference Series*, vol. 06, pp. 557–562, Jan. 2012, doi: 10.1142/s2010194512003777.

[54] G. Leftheriotis, P. Yianoulis, and D. Patrikios, "Deposition and optical properties of optimised ZnS/Ag/ZnS thin films for energy saving applications," *Thin Solid Films*, vol. 306, no. 1, pp. 92–99, Aug. 1997, doi: 10.1016/s0040-6090(97)00250-2.

[55] A. M. Al-Shukri, "Thin film coated energy-efficient glass windows for warm climates," *Desalination*, vol. 209, no. 1–3, pp. 290–297, Apr. 2007, doi: 10.1016/j.desal.2007.04.042.

[56] G. K. Dalapati et al., "Color tunable low cost transparent heat reflector using copper and titanium oxide for energy saving application," *Scientific Reports*, vol. 6, no. 1, p. 20182, Feb. 2016, doi: 10.1038/srep20182.

[57] M. F. Al-Kuhaili, "Transparent-conductive and infrared-shielding WO3/Ag/WO3 multilayer heterostructures," *Solar Energy*, vol. 250, pp. 209–219, Jan. 2023, doi: 10.1016/j.solener.2022.12.047.

[58] M. Diab and O. Alabbosh, "Studying of thickness effects on the optical and structural properties of ZNO/AG/ZNO multilayer thin films by using surface plasmon resonance," *Journals & Books Hosting (International Knowledge Sharing Platform)*, vol. 70, pp. 27–30, Jan. 2018.

[59] P. B. Johnson and R. W. Christy, "Optical constants of the Noble Metals," *Physical Review. B, Solid State*, vol. 6, no. 12, pp. 4370–4379, Dec. 1972, doi: 10.1103/physrevb.6.4370.

[60] B. G. Priyadarshini and A. K. Sharma, "Design of multi-layer anti-reflection coating for terrestrial solar panel glass," *Bulletin of Materials Science*, vol. 39, no. 3, pp. 683–689, May 2016, doi: 10.1007/s12034-016-1195-x.

[61] M. Forouzmehr et al., "Selective atomic layer deposition on flexible polymeric substrates employing a polyimide adhesive as a physical mask," *Journal of Vacuum Science & Technology a Vacuum Surfaces and Films*, vol. 39, no. 1, Dec. 2020, doi: 10.1116/6.0000566.

[62] W. A. Bryant, "The fundamentals of chemical vapour deposition," *Journal of Materials Science*, vol. 12, no. 7, pp. 1285–1306, Jul. 1977, doi: 10.1007/bf00540843.

[63] A.S.H. Makhlouf and I. Tiginyanu, 1st edition, *Nanocoatings and ultra-thin films: technologies and applications*. Elsevier p 3(2011).

[64] A. T. Salih, A. A. Najim, M. A. H. Muhi, and K. R. Gbashi, "Single-material multilayer ZnS as anti-reflective coating for solar cell applications," *Optics Communications*, vol. 388, pp. 84–89, Dec. 2016, doi: 10.1016/j.optcom.2016.12.035.

[65] A. Baptista, F. Silva, J. Porteiro, J. Míguez, and G. Pinto, "Sputtering Physical Vapour Deposition (PVD) Coatings: A Critical Review on Process Improvement and Market Trend Demands," *Coatings*, vol. 8, no. 11, p. 402, Nov. 2018, doi: 10.3390/coatings8110402.

[66] K. Wasa, I. Kanno and H. Kotera, *Handbook of sputter deposition fundamentals and applications for functional thin films, nano-materials and MEMS technology* (Elsevier), 2012

[67] S. M. Rossnagel, "Sputtering and sputter deposition," in *Handbook of Thin Film Deposition Processes and Techniques*. William Andrew Publishing, 2001, pp. 319–348.

[68] W. D. Westwood, "Glow discharge sputtering," *Progress in Surface Science*, vol. 7, no. 2, pp. 71–111, Jan. 1976, doi: 10.1016/0079-6816(76)90002-2.

[69] P. J. Kelly and R. D. Arnell, "Magnetron sputtering: a review of recent developments and applications," *Vacuum*, vol. 56, no. 3, pp. 159–172, Mar. 2000, doi: 10.1016/s0042-207x(99)00189-x.

[70] R. P. Howson, J. N. Avaritsiotis, M. I. Ridge, and C. A. Bishop, "Formation of transparent heat mirrors by ion plating onto ambient temperature substrates," *Thin Solid Films*, vol. 63, no. 1, pp. 163–167, Oct. 1979, doi: 10.1016/0040-6090(79)90120-2.

[71] M. I. Ridge, M. Stenlake, R. P. Howson, and C. A. Bishop, "The application of ion plating to the continuous coating of flexible plastic sheet," *Thin Solid Films*, vol. 80, no. 1–3, pp. 31–39, Jun. 1981, doi: 10.1016/0040-6090(81)90203-0.

[72] I. Dima, B. Popescu, F. Iova, and G. Popescu, "Influence of the silver layer on the optical properties of the TiO2/Ag/TiO2 multilayer," *Thin Solid Films*, vol. 200, no. 1, pp. 11–18, May 1991, doi: 10.1016/0040-6090(91)90026-t.

[73] C.-C. Lee, S.-H. Chen, and C.-C. Jaing, "Optical monitoring of silver-based transparent heat mirrors," *Applied Optics*, vol. 35, no. 28, p. 5698, Oct. 1996, doi: 10.1364/ao.35.005698

[74] R. W. Johnson, A. Hultqvist, and S. F. Bent, "A brief review of atomic layer deposition: from fundamentals to applications," *Materials Today*, vol. 17, no. 5, pp. 236–246, May 2014, doi: 10.1016/j.mattod.2014.04.026.

[75] J. O. Carlsson and P. M. Martin, *Handbook of Deposition Technologies for Films and Coatings*, 3rd ed. William Andrew Publishing, 2010, pp. 314–363

[76] X. Liu , " The design of ZnS/Ag/ZnS transparent conductive multilayer films," *Thin Solid Films*, vol. 441, no. 1–2, pp. 200–206, Jul. 2003, doi: 10.1016/s0040-6090(03)00141-x.

[77] S. M. A. Durrani, E. E. Khawaja, A. M. Al-Shukri, and M. F. Al-Kuhaili, "Dielectric/Ag/dielectric coated energy-efficient glass windows for warm climates," *Energy and Buildings*, vol. 36, no. 9, pp. 891–898, May 2004, doi: 10.1016/j.enbuild.2004.02.003.

[78] C. G. Granqvist, "Radiative heating and cooling with spectrally selective surfaces," *Applied Optics*, vol. 20, no. 15, p. 2606, Aug. 1981, doi: 10.1364/ao.20.002606.

[79] J. A. Pracchia and J. M. Simon, "Transparent heat mirrors: influence of the materials on the optical characteristics," *Applied Optics*, vol. 20, no. 2, p. 251, Jan. 1981, doi: 10.1364/ao.20.000251.

[80] H. Köstlin and G. Frank, "Optimization of transparent heat mirrors based on a thin silver film between antireflection films," *Thin Solid Films*, vol. 89, no. 3, pp. 287–293, Mar. 1982, doi: 10.1016/0040-6090(82)90601-0

[81] X. Zhang, "ZnS/Me heat mirror systems," *Solar Energy Materials and Solar Cells*, vol. 44, no. 3, pp. 279–290, Nov. 1996, doi: 10.1016/0927-0248(96)00060-8

[82] P. B. Johnson and R. W. Christy, "Optical constants of the Noble Metals," *Physical Review. B, Solid State*, vol. 6, no. 12, pp. 4370–4379, Dec. 1972, doi: 10.1103/physrevb.6.4370.

[83] F. P. Incropera and D. P. DeWitt, *Fundamentals of Heat and Mass Transfer*, 1st ed. New York, NY, USA: Wiley, 1996.

[84] A. Mutiari, T. Dimopoulos, M. Bauch, A. Mittal, M. Weil, and R. A. Wibowo, "Design and implementation of an ultrathin dielectric/metal/dielectric transparent electrode for Cu2ZnSnS4 thin-film photovoltaics," *Solar Energy Materials and Solar Cells*, vol. 230, p. 111247, Jun. 2021, doi: 10.1016/j.solmat.2021.111247.

[85]Ç. Çetinkaya, E. Çokduygulular, F. Güzelçimen, and B. Kınacı, "Functional optical design of thickness-optimized transparent conductive dielectric-metal-dielectric plasmonic structure," *Scientific Reports*, vol. 12, no. 1, p. 8822, May 2022, doi: 10.1038/s41598-022-13038-y

[86] Ren et al., "High-temperature thermal stable solar selective absorbing coating based on the dielectric-metal-dielectric structure," *Materials Today Physics*, vol. 34, p. 101092, Apr. 2023, doi: 10.1016/j.mtphys.2023.101092.

[87] W. Wang et al., "Construction of wear-resistant visible-infrared-compatible camouflage film and its spectral control mechanisms," *Infrared Physics & Technology*, vol. 140, p. 105383, Jun. 2024, doi: 10.1016/j.infrared.2024.105383

[88] M. P. Kumar, B. Nath, S. Satyanarayana, S. G. Siddanth, and P. C. Ramamurthy, "Ultra-thin dielectric-metal-dielectric as metal electrode alternative for bifacial perovskite and organic solar cells," *Materials Science and Engineering B*, vol. 319, p. 118350, Apr. 2025, doi: 10.1016/j.mseb.2025.118350

[89] L. Zhu, A.P. Raman and S. Fan 2015. Radiative cooling of solar absorbers using a visibly transparent photonic crystal thermal blackbody. *Proceedings of the national academy of sciences*, 112(40), pp.12282-12287.

[90] Z. Chen, L. Zhu, A. Raman, and S. Fan, "Radiative cooling to deep sub-freezing temperatures through a 24-h day–night cycle*," Nature Communications*, vol. 7, no. 1, p. 13729, Dec. 2016, doi: 10.1038/ncomms13729.

[91] Y. Huang et al., "Dual - Functional Metasurface toward Giant Linear and Circular Dichroism," *Advanced Optical Materials*, vol. 8, no. 11, Mar. 2020, doi: 10.1002/adom. 201902061

[92] J. Mandal et al., " Hierarchically porous polymer coatings for highly efficient passive daytime radiative cooling," *Science*, vol. 362, no. 6412, pp. 315–319, Sep. 2018, doi: 10.1126/science.aat9513

[93] Md. M. Hossain and M. Gu , " Radiative cooling: principles, progress, and potentials," *Advanced Science*, vol. 3, no. 7, p. 1500360, Feb. 2016, doi: 10.1002/advs.201500360.

[94] H. Wang et al. , "Solvent-engineering-processed CsPbIBr2 inorganic perovskite solar cells with efficiency of ∼11%," *Solar Energy Materials and Solar Cells*, vol. 238, p. 111640, Feb. 2022, doi: 10.1016/j.solmat.2022.111640.

[95] A. S. Rana, M. Zubair, A. Danner, and M. Q. Mehmood, "Revisiting tantalum based nanostructures for efficient harvesting of solar radiation in STPV systems," *Nano Energy*, vol. 80, p. 105520, Oct. 2020, doi: 10.1016/j.nanoen.2020.105520

[96] N. W. Khun and E. Liu, "Structures, adhesion strengths, and corrosion resistance of undoped, Nitrogen-Doped, and Platinum/Ruthenium/Nitrogen-Co-Doped Diamond-Like carbon thin films," *Journal of Materials and Engineering*, vol. 4, no. 1, pp. 10–28, Jan. 2026, doi: 10.61552/jme.2026.01.002.